ARTICLE

First-principles Studies on Electronic Structures of Ga-doped ZnO and ZnS

Ping Li[a*], Sheng-hua Deng[b], Li Zhang[a], Yi-bao Li[a], Jiang-ying Yu[a], Dong Liu[a]

a. Department of Mathematics and Physics, Anhui University of Architecture, Hefei 230022, China
b. School of Physics and Nuclear Energy Engineering, Beihang University, Beijing 100191, China

(Dated: Received on April 13, 2010; Accepted on September 8, 2010)

First-principles calculations have been performed to clarify the differences of the electronic structures of Ga-doped ZnO and ZnS. Results show the local density approximation and local density approximation+U calculations are in good qualitative agreement with each other. After doping, impurity states appear near the Fermi level in both ZnO and ZnS cases. When ZnO is doped, the impurity states are delocalized in the whole conduction band. On the contrary, when ZnS is doped, though the p state of Ga is also delocalized, the s state is localized near the Fermi level. Partial charge density distributions of the frontier orbital show the same information. After an exchange of the crystal structures of ZnO and ZnS, results remain unchanged. The localized Ga s state accounts for the bad electrical properties of Ga-doped ZnS.

Key words: First-principles, ZnS, ZnO, Doping

I. INTRODUCTION

ZnO in wurtzite structure is a direct and wide band gap (3.4 eV) semiconductor with large exciton binding energy (60 eV). It has become a promising material for optoelectronic devices, such as transparent field-effect transistors, light-emitting diodes (LED), solar cells and so on. So many studies about ZnO have been done [1−6]. Similarly, ZnS in zincblende structure is also a direct band gap semiconductor with a wide gap of 3.7 eV at room temperature, but there are some difficulties in the applications of ZnS because of its poor conductivity. It has been reported that the resistivity of ZnO doped by small amount of IIIA element impurities could decrease to about 0.3 mΩ cm [7−10]. On the contrary, the resistivity of doped ZnS is in the range of 1−100 Ωcm typically [11−13].

In order to clarify the great difference in the conductive behaviors between doped ZnO and ZnS, the gallium (Ga) atom is selected to be the dopant. In this work, the electronic structures including the total density of states (TDOS), partial density of states (PDOS), and the partial charge density of the frontier orbital have been studied by the first-principles method. An exchange of the crystal structures of ZnO and ZnS is finally considered.

II. MODEL AND METHOD

Ideal ZnO in wurtzite structure has a space group symmetry of P63/mc and C6v-4, with two O atoms and two Zn atoms in each primitive cell, and the cell parameters are a=b=324.9 pm, c=520.6 pm. ZnS in zincblende structure has a space group symmetry of F43m and T2d, with only one O atom and one Zn atom in each primitive cell, and the lattice constant is about 540.5 pm. Based on the primitive cells, supercells like Zn_8S_8, $Zn_{27}S_{27}$, $Zn_{16}O_{16}$, *etc.* are constructed. In our study, one of the zinc atoms in the supercells will be substituted by one Ga atom.

First-principles calculations based on the density functional theory (DFT) have been performed using the Vienna *ab initio* simulation package (VASP) code [14]. Ultrasoft pseudopotentials were used to describe the interactions between the atomic nucleus and valence electrons, and the local density approximation (LDA) was used to describe the exchange-correlation energy of electrons. Different k-point meshes in Brillouin zones were employed for the Brillouin zone integration for different primitive cells or supercells, which were 9×9×6 for Zn_2O_2, 4×4×2 for $Zn_{16}O_{16}$, 8×8×8 for Zn_1S_1, 4×4×4 for Zn_8S_8, and 3×3×3 for $Zn_{27}S_{27}$. Besides, the doped supercell used the same k-mesh as its undoped supercell. The selected energy cutoff for both pure and doped ZnO was 520 eV, and that for ZnS was 310 eV, which were confirmed to be large enough. In our calculations, the primitive cells and supercells were firstly relaxed until the force acting on each atom was less than 0.01 eV/Å, and the calculated lattice parameters were in good agreement with the experimental values. Then the band structures, the TDOS, the partial charge density of the frontier orbital, and the PDOS of the dopant atom were calculated.

*Author to whom correspondence should be addressed. E-mail: liping@aiai.edu.cn

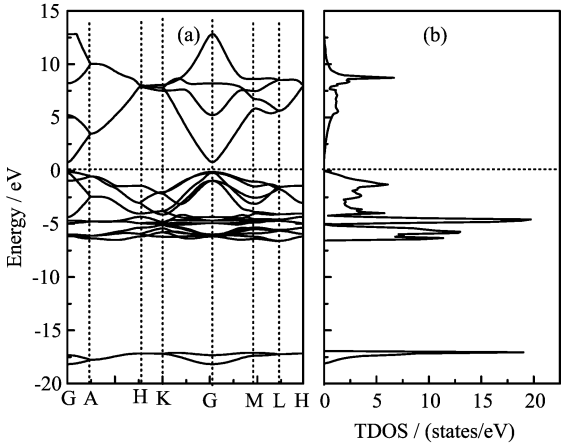

FIG. 1 Band structure (a) and TDOS (b) of Zn_2O_2 from LDA results.

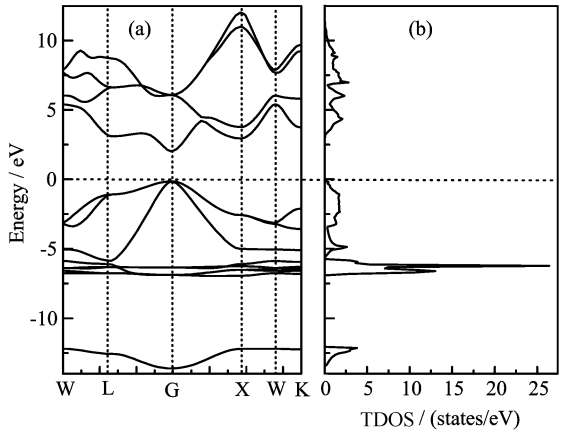

FIG. 2 Band structure (a) and TDOS (b) of Zn_1S_1 from LDA results.

TABLE I Lattice parameters of primitive ZnO with experiment data and calculation values.

	a/pm	c/pm	c/a
$Zn_2O_2{}^{Exp.}$	324.9	520.6	1.602
$Zn_2O_2{}^{Cal.}$	324.1	513.7	1.585
$Zn_{15}GaO_{16}{}^{Cal.}$	320.8	515.3	1.606

III. RESULTS AND DISCUSSION

A. Pure primitive cells

The calculated lattice parameters of the pure and doped ZnO are shown in Table I. For the pure and doped ZnS, the calculated lattice parameters of Zn_1S_1, Zn_7GaS_8, and $Zn_{26}GaS_{27}$ are 531.0, 534.4, and 532.2 pm, respectively, compared with the experiment lattice parameters of Zn_1S_1 (540.4 pm). The parameters of supercells have been converted for the respective primitive cells. It is obvious that the calculated values are in good agreement with the experimental data, which assures the reliability of our method.

The calculated band structure and TDOS of Zn_2O_2 and Zn_1S_1 primitive cells are shown in Fig.1 and Fig.2 respectively, where the Fermi level is specified to zero.

Several points of similarity should be noted for Fig.1 and Fig.2. Firstly, it's obvious that the bottom of the conduction band and the top of the valence band are at the same k-point (G) for both of the cells, indicating that both ZnO and ZnS are direct gap semiconductors. However, the calculated band gap of ZnO is about 0.83 eV and that of ZnS is 1.89 eV, only 24% and 51% of the experimental data, respectively. The underestimation of semiconductor band gaps is a common problem of LDA, and it can be partly corrected by LDA+U. The second similar point is that an isolated band locates deeply into the valence band for the both, about -18 and -12 eV for Zn_2O_2 and Zn_1S_1 respectively. However, the bands are so isolated and so far away from the other bands that we will pay little attention to it. Finally, the valence band of both Zn_2O_2 and Zn_1S_1 can be divided into two parts. For Zn_2O_2, the lower part is from -6.3 eV to -4.2 eV and the upper part from -4.2 eV to about -0.03 eV, while that for Zn_1S_1 is from -6.4 eV to -5.6 eV and from -5.6 eV to -0.02 eV, respectively. Though there are so many similarities, at least one ting is different. The conduction band of Zn_2O_2 is sharp and localized, but that of Zn_1S_1 changes continuously and gently.

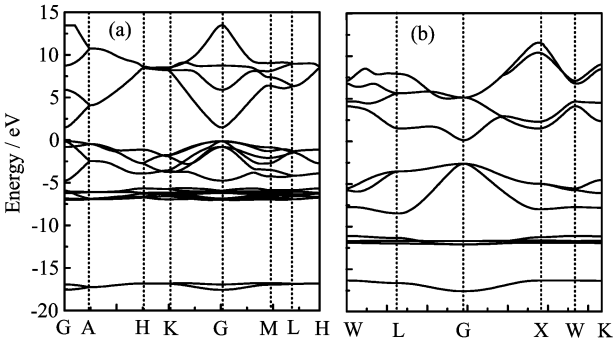

FIG. 3 Band structure of ZnO (a) and ZnS (b) from LDA+U results.

In order to testify the reliability of our results qualitatively, LDA+U calculations were performed for both ZnO and ZnS primitive cells. Figure 3 show the band structures of ZnO and ZnS from LDA+U calculations, respectively.

Firstly, the plots of LDA+U agree qualitatively with those of LDA shown in Fig.1(a) and Fig.2(a), meaning the qualitative reliability of the LDA results. Secondly, the band gaps are partly corrected by LDA+U. The LDA+U gap of ZnO is corrected to be 1.49 eV, compared to 0.83 eV from LDA calculations, and that of ZnS is 2.23 eV compared to the LDA value of 1.89 eV. The calculated LDA+U gap of ZnO in this work agrees well with the value reported by Anderson *et al.* [15], who have reported a calculated value of 1.51 eV using

DOI:10.1088/1674-0068/23/05/527-532

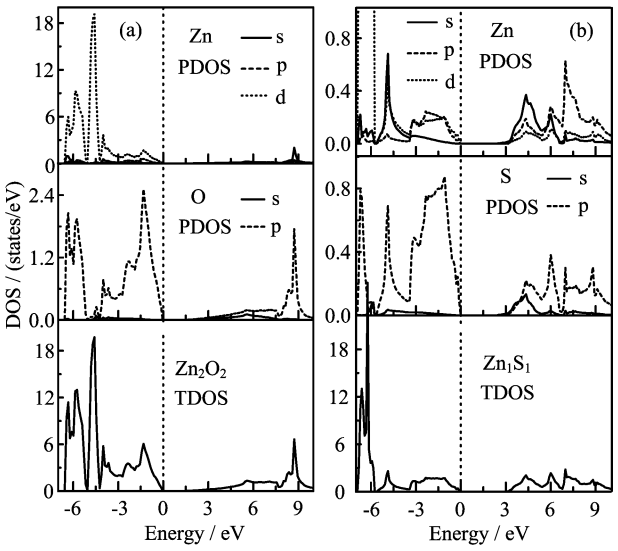

FIG. 4 TDOS and PDOS of Zn_2O_2 (a) and Zn_1S_1 (b) from LDA results.

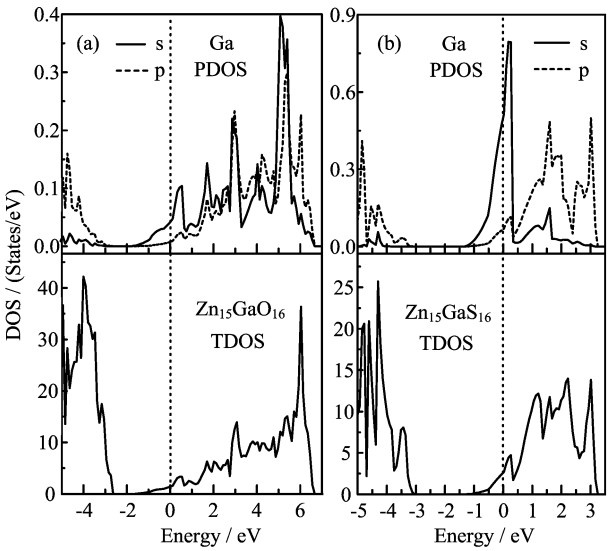

FIG. 5 TDOS and PDOS of $Zn_{15}GaO_{16}$ and Zn_7GaS_8 from LDA results.

the same method. Though the LDA+U gaps are still smaller than the experimental values, they are much better than the LDA results.

Figure 4 shows the LDA TDOS and PDOS of Zn_2O_2 and Zn_1S_1 near the Fermi level. From the two plots we can see that for both Zn_2O_2 and Zn_1S_1, the lower valence band is mainly contributed by the 3d states of Zn, and the upper comes mainly from the 2p states of O or the 3p states of S, respectively. However, in the conduction band region, the O2p orbital is more localized than the S3p orbital in the same region, indicating that the O2p orbital is a tight-binding state and contributes little to the conductivity of ZnO.

B. Doped situations

When one Zn atom of the supercell is substituted by one Ga atom, changes to the lattice happen to both the doped ZnO and ZnS, as listed in Table I and Table II. From the tables, we can see the changes are small for the both cases, and can not be explained simply by the difference of atomic or ionic radius between the Ga and Zn atoms. Based on the relaxed supercells, the electronic structures of Ga-doped ZnO and ZnS have been calculated.

Figure 5 show the TDOS and PDOS of $Zn_{15}GaO_{16}$ and Zn_7GaS_8, respectively. Firstly, in the case of ZnO doping, Fermi level shifts upward into the conduction band, accounting for the good conductivity of Ga-doped ZnO. Secondly, in the both doping cases, the p states of the Ga atom in the conduction band are delocalized, while the s state is quite different. The s state of Ga is delocalized in the case of $Zn_{15}GaO_{16}$, but localized in the case of Zn_7GaO_8. To compare the TDOS of Zn_7GaS_8 with the PDOS of the Ga atom shown in Fig.5, we can see that an impurity state ranging from -0.8 eV to 0.4 eV appears near the bottom of the conduction band for doped ZnS. The impurity state is localized, and the s state of Ga is just located sharply in this region, only with a small part escaping from the region. So the localized state around Fermi level acts as a potential well and it traps the s electrons of the Ga atom. It well prevents the s electrons from getting into the conduction band and results in the poor electrical conductivity of doped ZnS.

From the discussions above, the delocalized states of the Ga atom in the doped ZnO accounts for its good electrical properties, while the localized s state of Ga accounts for the bad electrical properties of the doped ZnS. However, it is a little different from the results reported by Yojiimai *et al.* [16], who has not relaxed the supercells.

In the doping cases, the LDA+U calculations were also performed to testify the qualitative reliability of our LDA calculations. The TDOS and the PDOS of the LDA+U calculations corresponding to the Fig.5 are shown in Fig.6.

Figure 6 is in good qualitative agreement with Fig.5. Fermi level shifts upward into the conduction band, and the TDOS value at Fermi level is about 3.5 states/eV. From Fig.6, the PDOS of the Ga atom is delocalized in the conduction band, and the Ga s and p states are a resonance in the conduction band. The results above mean better electrical properties of Ga-doped ZnO. For Ga-doped ZnS, things are different. From TDOS shown in Fig.6(b), an impurity state appears near the Fermi level with a TDOS value of 2.7 states/eV, which is much smaller than that of doped ZnO shown in Fig.6(a). Besides, though the Ga p state is a resonance in the conduction band, the Ga s states is localized near the Fermi level. The two points above account for the poor con-

DOI:10.1088/1674-0068/23/05/527-532

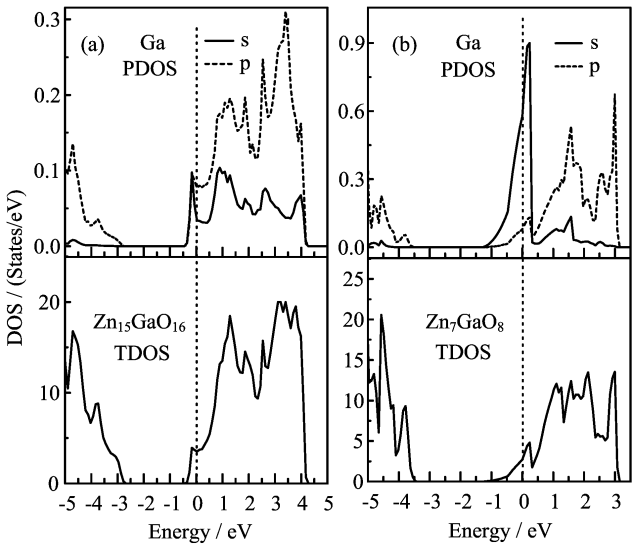

FIG. 6 TDOS and PDOS of $Zn_{15}GaO_{16}$ (a) and Zn_7GaS_8 (b) from LDA+U results.

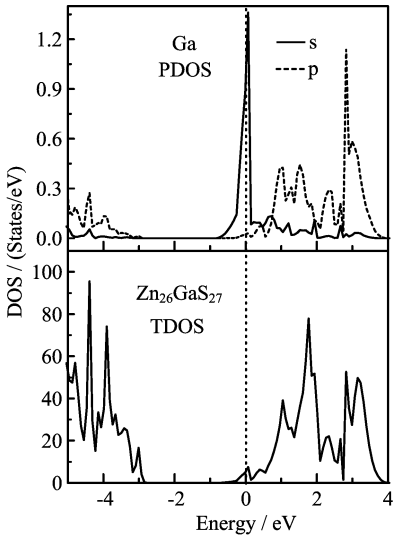

FIG. 7 TDOS and PDOS of $Zn_{26}GaS_{27}$ from LDA results.

ductivity of doped ZnS. It is obvious that, the LDA+U results for doped ZnS are also in good qualitative agreement with the results for LDA.

From the above analyses of the LDA and LDA+U results of doped ZnO and ZnS, it can be concluded that LDA can give qualitatively consistent results with LDA+U, though some quantitative results may be different. So in the following parts, only the LDA calculations and discussions will be performed, and the results are qualitatively reliable.

In Fig.5(b), the doping content of Zn_7GaS_8 is 6.25%, and this concentration is high more or less, so a larger supercell or lower doping content is used to testify the convergence of the doping behavior.

Figure 7 shows the TDOS and PDOS of $Zn_{26}GaS_{27}$, in which the doping content decreased to 1.85%. One can see that the curve shape shown in the Fig.7 is almost the same as that shown in Fig.5(b). But not only that, the Ga s state in $Zn_{26}GaS_{27}$ is sharper and more delocalized than that in Zn_7GaS_8. Besides, the Ga p state extends widely in the whole conduction band. All of these indicate the convergence of impurity behaviors. It can also be concluded that the localized state of the Ga s orbital accounts for the poor conductive behavior of doped ZnS.

In order to see clearly the space distributions of the frontier orbital, Fig.8 gives the partial charge density of the frontier band structures, *i.e.*, the charge density corresponding to four or five lines of each band edges (valence band maximum and conduction band minimum). Figure 8(a) shows the charge density of pure ZnO. It's clear that the charge distributions are characterized by ionic character, but a few directional properties are also exhibited. So chemical bonds mixed ionic-covalent character are formed between the O and Zn atoms in ZnO crystal, and of course the ionic character is main. Figure 8(b) shows the doping case of ZnO, and it is so clear that the space distributions of the electrons change a lot compared to the pure case. The most obvious change is that the frontier orbital of the Ga atom is spatially delocalized, exhibiting a metallic behavior. This is in agreement with the PDOS curves of the doped ZnO, which are characterized by delocalization and shown in the Fig.5(a) and Fig.6(a). We think that it is the delocalized distributions of the Ga frontier orbital that result in the good electrical transportation property of doped ZnO.

Figure 8(c) shows the charge density distributions of the frontier orbital of ZnS. The characteristics of the Fig.8(c) are very similar to those of Fig.8(a), so the S−Zn bonds in ZnS crystal also show mixed ionic-covalent character, and of course again, the ionic character is main. When ZnS is doped by Ga atom, changes to the charge density distributions are small, as shown in the Fig.8(d). It can be seen the frontier Ga orbital is localized around the Ga atomic space, forming ionic bonds with the adjacent O atoms. The above characteristics are also in agreement with the PDOS of the Ga atom in doped ZnS shown in Fig.5(b), Fig.6(b), and Fig.7. However, it is very different from the case in Fig.8(b), where the Ga orbital is very delocalized. So we think that it is the localized frontier Ga orbital accounts for the poor transportation properties of doped ZnS.

As discussed above, we have known that the good electrical conductivity of the Ga-doped ZnO is mainly because of the delocalized behaviors of the impurity states, which are hybridized well with the states of the host material in conduction band. On the contrary, in Ga-doped ZnS, the impurity states, especially the s states of the Ga atom, are quite localized near the Fermi level. The localized states prevent the electrons,

DOI:10.1088/1674-0068/23/05/527-532

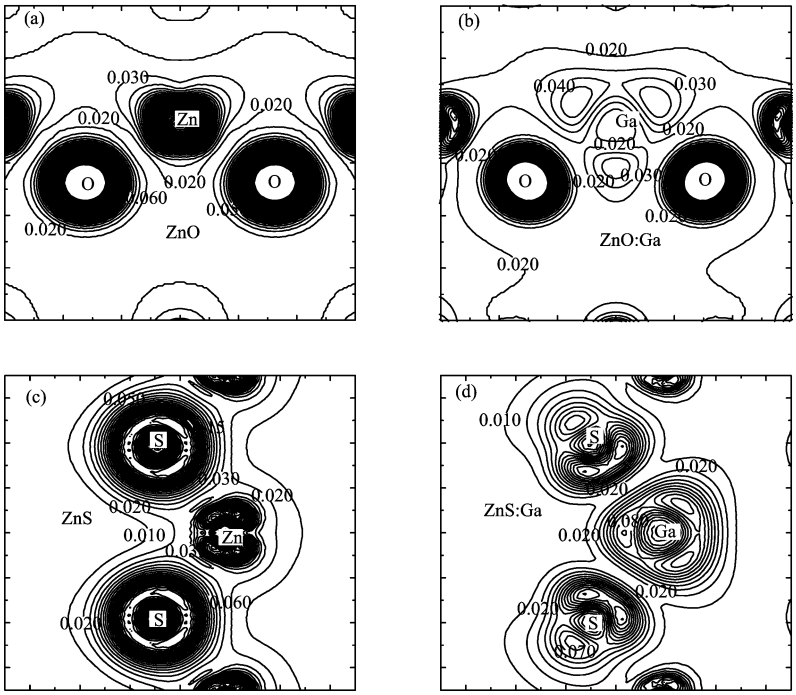

FIG. 8 Partial charge density distributions of the frontier orbital of pure ZnO (a), Ga-doped ZnO (b), pure ZnS (c) and Ga-doped ZnS (d). The interval of the contour lines is 0.01 e/Å^3.

especially the Ga s electrons, from escaping into the conduction band, and results in the poor conductivity of Ga-doped ZnS.

C. Exchanging structures

Finally, we performed calculations for exchanging crystal structures to investigate whether the doping behavior is structure-dependent or not.

A hypothetical zincblende structure for Zn_7GaO_8 and a wurtzite structure for $Zn_{15}GaS_{16}$ are constructed in this work. For the hexagonal ZnS, lattice parameters of high temperature phase [17] (a=382.3 pm, c=626.1 pm) are adopted, and parameters of a=370.0 pm and c=616.4 pm are obtained after relaxation. For cubic ZnO, a lattice parameter of 456.7 pm is adopted to keep the volumes equal between the hypothetical and the real hexagonal primitive cells, and no relaxation is considered. The TDOS and the PDOS of the hypothetical cubic Zn_7GaO_8 and hexagonal $Zn_{15}GaS_{16}$ are shown in Fig.9. Figure 9(a) shows a widely extended 3s state of the Ga atom in the whole conduction band, which means a good hybridization with the native conduction band. On the contrary, Figure 9(b) shows a localized 3s state of the Ga atom near the Fermi level, which is almost the same as doped ZnS in zincblende structure. So it seems that exchanging structure does not improve the poor conductive behaviors of doped ZnS.

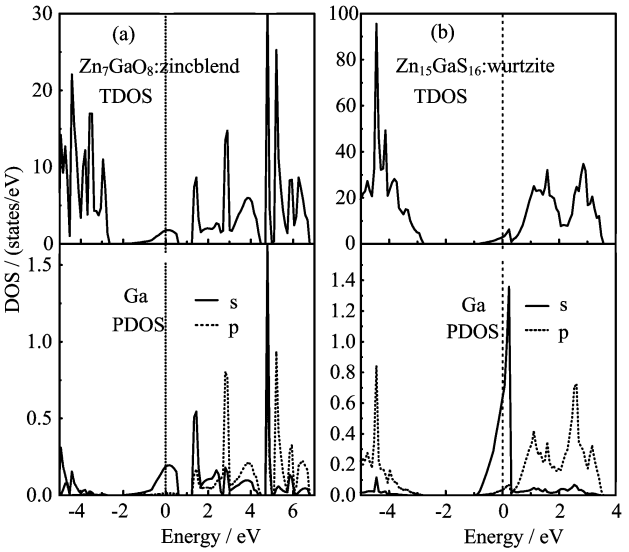

FIG. 9 TDOS and PDOS of hypothetical zincblende Zn_7GaO_8 (a) and wurtzite $Zn_{15}GaS_{16}$ (b) from LDA results.

IV. CONCLUSION

To clarify the electronic structure differences of Ga-doped ZnO and ZnS, first-principles calculations, including the LDA and LDA+U calculations, have been performed, and the following conclusions can be derived. (i) The LDA and LDA+U calculations are in good qualitative agreement with each other, but the

DOI:10.1088/1674-0068/23/05/527-532

LDA+U band gaps are more reasonable compared to the respective experimental values. (ii) When ZnO is doped, the impurity states are delocalized in the conduction band. On the contrary, when ZnS is doped, the Ga s state is quite localized near the conduction band edge. (iii) The partial charge density of frontier orbital shows that chemical bonds mixed ionic-covalent character are formed in both ZnO and ZnS crystals. When ZnO is doped, the electrons of the dopant atom are delocalized, exhibiting good transportation properties. However, when ZnS is doped, the electrons of the Ga atom are quite localized, indicating bad transportation properties.

V. ACKNOWLEDGMENTS

This work was supported by the Foundation for the Excellent Youth Scholars of Anhui Education Office (No.2009SQRZ097ZD) and the Foundation of Anhui Province Education Bureau (No.2006KJ270B).

[1] X. Su, P. Si, Q. Hou, X. Kong, and W. Cheng, Physica B **404**, 1794 (2009).
[2] S. Limpijumnong, X. Li, S. Wei, and S. B. Zhang, Physica B **376**, 686 (2006).
[3] C. G. Van de Walle, Phys. Rev. Lett. **85**, 1012 (2000).
[4] S. Limpijumnong, X. Li, S. H. Wei, and S. B. Zhang, Appl. Phys. Lett. **86**, 211910 (2005).
[5] X. Duan, Y. Zhao, and R. Yao, Solid State Commun. **147**, 194 (2008).
[6] M. G. Wardle, J. P. Goss, and P. R. Briddon, Phys. Rev. Lett. **96**, 205504 (2006).
[7] T. Minami, H. Nanto, and S. Takata, Jpn. J. Appl. Phys. **23**, L280 (1984).
[8] J. Hu and R. G. Gordon, J. Appl. Phys. **71**, 880 (1992).
[9] H. Sato, T. Minami, S. Takata, T. Miyata, and M. Ishii, Thin Solid Films **236**, 14 (1993).
[10] B. Szyszka, Thin Solid Films **351**, 164 (1999).
[11] L. C. Olsen, R. C. Bohara, and D. L. Barton, Appl. Phys. Lett. **34**, 528 (1979).
[12] C. B. Thomas, H. S. Errhal, A. J. Warren, and J. M. Gallego, Appl. Phys. Lett. **38**, 736 (1981) .
[13] S. Iida and S. Suzuki, J. Non-Cryst. Solids **59/60**, 633 (1983).
[14] G. Kress and J. Furthmuller, Phys. Rev. B **54**, 11169 (1996).
[15] J. Anderson, G. Chris, and van De Walle, Phys. Rev. B **76**, 165202 (2007).
[16] Yojimai and A. Watanabe, J. Mater. Sci. Mater. Electron. **14**, 149 (2003).
[17] R. R. Reever and G. W. Powell, J. Appl. Phys. **38**, 1531 (1967).

DOI:10.1088/1674-0068/23/05/527-532